RHPN1-AS1 promotes ovarian carcinogenesis by sponging miR-6884-5p thus releasing TOP2A mRNA

SHOUBIN CUI and FENGLING LI

Department of Gynaecology and Obstetrics, Yantai Affiliated Hospital of Binzhou Medical University, Yantai, Shandong 264100, P.R. China

Received August 28, 2020; Accepted July 19, 2021

DOI: 10.3892/or.2021.8172

Abstract. Ovarian cancer, a severe lethal gynecological malignancy, is characterized by both high morbidity and mortality. Long noncoding RNAs (lncRNAs) have recently caused extensive concern due to their regulatory function in various human tumors. There are a mounting number of lncRNAs that are in extreme need of research, serving as biomarkers for diagnosis and therapy for ovarian cancer. In the present study, RT-qPCR was employed to detect how Rhophilin Rho GTPase binding protein 1 antisense RNA1 (RHPN1-AS1), miR-6884-5p and DNA topoisomerase IIα (TOP2A) are expressed in ovarian cancer tissues or cell lines. BrdU, MTT, colony formation and cell adhesion assays, caspase-3 activity, flow cytometry and wound healing assay were employed to assess cell proliferation, viability, colony number, adhesion, apoptosis and migration in ovarian cancer, respectively. RHPN1-AS1 was determined to be enriched in ovarian cancer tissues and cell lines. Silencing of RHPN1-AS1 was reported to increase cell apoptosis and impair cell proliferation, viability, colony number, adhesion and migration *in vitro*. Furthermore, RHPN1-AS1 was able to sponge miR-6884-5p which directly targets TOP2A in ovarian cancer. Notably, silencing of RHPN1-AS1 functionally reversed the oncogenic effect induced by the miR-6884-5p inhibitor, while the miR-6884-5p inhibitor markedly restored the inhibition of ovarian carcinogenesis modulated by silencing TOP2A in ovarian cancer. RHPN1-AS1 was found to promote ovarian carcinogenesis via sponging miR-6884-5p thus releasing TOP2A, and RHPN1-AS1 may act as a promising biomarker for the prognosis and therapy of ovarian cancer.

Correspondence to: Dr Fengling Li, Department of Gynaecology and Obstetrics, Yantai Affiliated Hospital of Binzhou Medical University, 717 Jinbu Street, Muping, Yantai, Shandong 264100, P.R. China
E-mail: lifengling71@163.com

Abbreviations: lncRNAs, long noncoding RNAs; RHPN1-AS1, Rhophilin Rho GTPase binding protein 1 antisense RNA1; miRNA, microRNA; TOP2A, DNA topoisomerase IIα; logFC, log fold change; DEGs, differentially expressed genes; NC, negative control; si, silencing plasmids

Key words: ovarian cancer, oncogene, RHPN1-AS1, miR-6884-5p, TOP2A

Introduction

Ovarian cancer, characterized by both high morbidity and high mortality, has been regarded as the most lethal gynecological malignancy worldwide (1,2). Resulting from the lack of specific signs or symptoms at the early stages, most women are diagnosed at advanced stages. The 5-year survival rate of ovarian cancer is only about 30% (3). With the advancement of modern medical technologies, platinum and taxane derivatives are applied for the chemotherapy of ovarian cancer (4). However, with easy metastasis and recurrence, a satisfactory therapeutic effect for ovarian cancer cannot be achieved (5). Therefore, there is an urgent need to discover novel biomarkers to be utilized for therapeutic methods for ovarian cancer.

Long noncoding RNAs (lncRNAs), as transcript, are made up of more than 200 nucleotides (6). Although lncRNAs lose the ability of coding proteins, they are still reported as truly functional biomolecules (7). lncRNAs have been identified as competing endogenous (ce)RNAs to interact with miRNAs, thereby carrying out regulatory functions in tumor biological behaviors, including cell apoptosis, viability and metastasis (8-10). Rhophilin Rho GTPase Binding Protein 1 antisense RNA1 (RHPN1-AS1) is affiliated with the lncRNA class. Based on our search results for functions of RHPN1-AS1 in cancer, there are 9 articles exploring the relationship between RHPN1-AS1 and human tumors. The role of RHPN1-AS1 in human tumors remains controversial. Specifically, lncRNA RHPN1-AS1 has been identified as an oncogene in cervical cancer (11), gastric cancer (12), hepatocellular carcinoma (13) and colorectal cancer (14). Contrarily, RHPN1-AS1 was found to act as a suppressor in breast cancer (15) and non-small cell lung cancer (16). However, the role of RHPN1-AS1 in ovarian cancer is still in need of relevant reports.

Compared with lncRNAs, microRNAs (miRNAs) are defined as shorter RNAs without the function of coding proteins (17). As post-transcriptional regulators, miRNAs functionally bind to the target mRNA, which leads to translation inhibition of the target mRNA. Thus, miRNAs could participate in cancer cellular biological processes (18-20). Additionally, miRNAs could be sponged and negatively regulated by corresponding lncRNAs to exert regulatory

functions in human tumors (16). Therefore, neither the effects of miR-6884-5p nor the interactive relationship between miR-6884-5p and RHPN1-AS1 has been elaborated in ovarian cancer.

DNA topoisomerase IIα (*TOP2A*), a protein coding gene, is located on chromosome 17q22.2 and includes 36 exons. It encodes a DNA topoisomerase, which acts as an enzyme to control and alter the topologic states of DNA during transcription. In the past three decades, the function of *TOP2A* in various human tumors has brought about widespread attention worldwide. Of the more than two hundred articles that have reported the role of *TOP2A* in diverse cancers, 20 literatures have studied the relationship between *TOP2A* and ovarian cancer (22-24). But none has explored the regulatory relationship between *TOP2A* and miRNAs in ovarian cancer.

In the present, the regulatory function mechanism of RHPN1-AS1/miR-6884-5p/*TOP2A* in regards to ovarian cancer was explored by cellular behavioral experiments. We put forward a hypothesis that upregulation of RHPN1-AS1 functionally repressed cell apoptosis and enhanced the ability of cell proliferation, viability, adhesion as well as migration in ovarian cancer by sponging miR-6884-5p and releasing *TOP2A*. Consequently, RHPN1-AS1 may serve as a promising biomarker for ovarian cancer.

Materials and methods

Bioinformatics analysis. GSE119056 (25) and GSE23392 (26) downloaded from Gene Expression Omnibus (GEO) datasets (27) included the mRNA expression profiles. With log fold change (logFC) ≥1.5 and P-value <0.01, the upregulated differentially expressed genes (DEGs) were screened out. Then, the overlapping DEGs from GSE119056 and GSE23392 were uploaded to STRING to perform the networking analysis. Gene Expression Profiling Interactive Analysis (GEPIA, http://gepia.cancer-pku.cn/index.html) was used to show the expression of RHPN1-AS1, our gene of interest, in ovarian cancer. Finally, the key miRNA binding to RHPN1-AS1, our gene of interest, was found by ENCORI Starbase (http://starbase.sysu.edu.cn/panCancer.php) and TargetScan (http://www.targetscan.org/vert_71/), respectively.

Tissue samples. A total of 37 tumor tissues and corresponding adjacent normal tissues from ovarian cancer patients were obtained from Yantai Affiliated Hospital of Binzhou Medical University between June 2019 and December 2020. The age range of the 37 patients was 45-70 years with the 60 years mean age. Our study methodologies conformed to the standards set by the Ethics Committee of Yantai Affiliated Hospital of Binzhou Medical University (approval no. 20190601001, Yantai, Shandong, China). All the patients provided their written informed consent. The clinical characteristics of the 37 patients are listed in Table I.

Cell culture. Ovarian cancer cell lines (SKOV3, OVCAR3, CaoV3 and OV90) and normal ovarian epithelial cells (HOSE) collected from the American Type Culture Collection (ATCC) were cultured in RPMI-1640 medium (Sigma; Merck KGaA) with 10% (v/v) fetal calf serum (Invitrogen; Thermo Fisher Scientific, Inc.) under 5% CO_2 at 37˚C.

Fluorescence in situ hybridization (FISH). The lncRNA RHPN1-AS1 probe was designed and synthesized by Guangzhou RiboBio Co., Ltd. (China). The cells were cultured in a 24-well plate for 24 h incubation. Then, the cells were immobilized with 4% paraformaldehyde for 10 min, and treated with 0.5% Triton X-100 permeate solution for 5 min. After preheating the pre-hybridized solution at 37˚C, the pre-hybridized solution was added to the cells to incubate cells for 30 min. The lncRNA RHPN1-AS1 probe diluted by the hybrid solution at the ratio of 1:50 was added into the culture plate at 200 μl per well for incubation overnight at 37˚C. The next day, removing the hybridized mixture, the saline sodium citrate (SSC) was preheated at 45˚C, and the cells were washed in the order of 4X SSC, 2X SSC, and 1X SSC for three times each. Next, 20 μl DAPI was added to each well for staining at room temperature for 10 min. After washing with PBS, the slides were fixed with anti-fluorescence quenching sealing tablet, and the images were captured using fluorescence microscope (Olympus IX70; Olympus) under x400 magnification.

Cell transfection. The RHPN1-AS1 silencing plasmids, miR-6884-5p inhibitor and TOP2A silencing plasmids and their corresponding negative control (NC) were constructed and obtained from Guangzhou RiboBio Co., Ltd. Before transfections, the cells were cultured in a 96-well-plate ($1x10^5$/ml), a 12-well-plate ($1x10^6$/ml) or a 6-well-plate ($2.5x10^6$/ml) to a density of 50%. Lipofectamine 2000 (Invitrogen; Thermo Fisher Scientific, Inc.) was applied to conduct cell transfections. As described in the protocol, the transfection concentrations of RHPN1-AS1 silencing plasmids, *TOP2A* silencing plasmids and their NC were 100 ng for a 96-well plate, 1,000 ng for a 12-well-plate and 2,500 ng for a 6-well-plate. The primer sequence of RHPN1-AS1 silencing plasmids, miR-6884-5p inhibitor and *TOP2A* silencing plasmids are showed in Table SI. Transfection concentrations of the miR-6884-5p inhibitor were 3 pmol for a 96-well-plate, 30 pmol for a 12-well-plate and 75 pmol for a 6-well-plate. After transfection for 48 h, the transfection efficiency was detected by RT-qPCR. The sequences of all the constructed vectors are shown in Table SI.

RT-qPCR. Total RNA Extraction Kit (Solarbio, China) was used to extract total RNAs from the tissues and cells. The cDNAs were synthesized by PrimeScript RT reagent kit (Takara Bio, Inc.). RT-qPCR was performed by TB Green® Premix Ex Taq II kit (Takara Bio, Inc.). β-actin was applied as the reference gene for RHPN1-AS1 and *TOP2A*, and U6 was the reference gene for miR-6884-5p. $2^{-\Delta\Delta Cq}$ method (28) was applied for the calculation of the relative expression level. The sequence information of primers is listed in Table II.

Subcellular fractionation. Nuclear and cytoplasmic fractionations of SKOV3 and OVCAR3 cells were separated with NE-PER Nuclear and Cytoplasmic Extraction Kit (Thermo Fisher Scientific, Inc.). RHPN1-AS1 expression was detected using RT-qPCR. GAPDH/U6 was the cytoplasmic/nuclear control.

BrdU assay. BrdU assay was conducted by the 5-bromo-2'-deoxyuridine (BrdU) kit (YEASEN, China). SKOV3 and OVCAR3 cells were seeded in 96-well plates. After a 48-h

Table I. Baseline characteristic of the patients with ovarian cancer (n=37).

Characteristics	Data values n (%)
Age at diagnosis (years)	
Age >60	21 (56.76)
Age ≦60	16 (43.24)
Tumor size (cm)	
≦10	20 (54.05)
>10	17 (45.95)
Tumor type	
Invasive	22 (59.46)
Borderline	12 (32.43)
Unknown	3 (8.11)
Histological type	
Serous	27 (72.97)
Endometrioid	3 (8.11)
Mucinous	6 (16.22)
Clear cell	1 (2.70)
FIGO stage	
I/II	19 (51.35)
III/IV	18 (48.65)
Pathological grade	
G1+G2	23 (62.16)
G3	14 (37.84)

transfection, 100 μl BrdU liquid was used to treat the cells in each well for a 2-h incubation. The absorbance at 450 nm was determined in a microplate reader (BioTek).

MTT assay. MTT cell proliferation and cytotoxicity assay kit (Sangon Biotech Co., Ltd.) was applied to determine the cell viability of SKOV3 and OVCAR3 cells. The cells were incubated for 0, 24, 48 and 72 h transfection. Before determination, 10 μl MTT reagent was used to treat the cells in each well. After a 4-h incubation, the absorbance was monitored at 570 nm using a microplate reader (BioTek).

Colony formation assay. The transfected cells were seeded into a 6-well cell culture plate at $1x10^3$ cells/well to culture for 2 weeks. After culturing, the medium was removed and washed with PBS for 3 times. Then, the cells were fixed with 1 ml methanol for 20 min and stained with 0.1% crystal violet solution for 30 min. After that, the remaining crystal violet solution was slowly washed with running water. Finally, the cells were photographed with an optical microscope with x200 magnification, and the number of clones was counted.

Cell adhesion assay. CultreCoat® BME 96 Well Cell Adhesion Assay Kit (Trevigen, Inc.) was used to carry out this detection. A 96-well-plate was coated with Laminin-1 overnight. The plate was washed by washing buffer for twice. Then the plate was blocked with blocking buffer at 37˚C for 1 h. An amount of 50 μl cells after a 48-h transfection was added into each well for an incubation for 30 min. The cells were fixed by 4% paraformaldehyde. Crystal violet (0.5%) was added to stain the cells. After washing with washing buffer, the plate was turned upside down and dried up completely, and 2% SDS was added for a 30-min incubation. Finally, the absorbance was determined at 570 nm by a microplate reader (BioTek).

Caspase-3 activity assay. Caspase-3 activity assay kit (Cell Signaling Technology, Inc.) was used for the analysis of caspase-3 activity of SKOV3 and OVCAR3 cells after transfection for 72 h. Based on the protocol, cells were digested by trypsin and collected by centrifuging at 630 x g for 5 min. Supernatant was discarded and cells were resuspended gently and counted. At the proportion of 50 μl lysate per $2x10^6$ cells, the cells were treated by precooled lysis buffer. The cells were treated with a centrifugation at 4˚C at 3,780 x g for 10 min. Supernatant was carefully absorbed and transferred to a new EP tube. Ac-DEVD-pNA was added for a 4-h incubation. The absorbance was determined at 405 nm by a microplate reader (BioTek, USA). The sample OD value/blank group OD value ratio was used to determine caspase-3 activation.

Flow cytometric assay. The apoptosis rate was detected by Annexin V-FITC/PI apoptosis kit (eBioscience; Thermo Fisher Scientific, Inc.). SKOV3 and OVCAR3 cells after transfection for 48 h were seeded into 6 well plates at $2x10^5$ cells/well. After the cell confluence reached 80%, the cells were collected. Then, 400 μl premixed 1X buffer binding was added into the cells, and the cell suspension was transferred into a flow tube. Next, into the cell suspension in the flow tube was added 5 μl of Annexin V-FITC and 5 μl of propidium iodide (PI) to incubate for 15 min in the dark. After incubation, the cells were analyzed using the BD FACScalibur Flow cytometry (BD Biosciences), which is equipped with Cell Quest software version 5.1 (BD Biosciences).

Wound healing assay. Wound healing assay was applied to demonstrate the migration ability of the SKOV3 and OVCAR3 cells. The cells after a 48-h transfection were seeded in 6-well plates at the density of $2x10^5$ cells/well. When the cell confluence was more than 90%, 200-μl pipette tips were used to make the wounds in the middle of the 6-well plates plated, and the wounds at 0 h were photographed using an optical microscope. After incubation with serum-free medium for 24 h, the wounds at 24 h were also photographed using an optical microscope. The cell migration rate was calculated by the change of wounds width at 0 and 24 h.

Dual luciferase reporter assay. SKOV3 and OVCAR3 cells were transfected with RHPN1-AS1 wild-type (psiCHECK2-RHPN1-AS1-WT, WT-lnc), RHPN1-AS1 mutant-type (psiCHECK2-RHPN1-AS1-MUT, MUT-lnc), *TOP2A* 3'UTR wild-type (psiCHECK2-TOP2A-WT, WT) or *TOP2A* 3'UTR mutant-type (psiCHECK2-TOP2A-MUT, MUT) from Guangzhou RiboBio Co., Ltd., which was transfected with miR-6884-5p mimic or mimic negative control (NC). Dual-Luciferase Reporter Assay System (Promega Corp.) was applied to detect the firefly and Renilla luciferase activities. Relative luciferase activity was normalized to the firefly luciferase internal control. Fluorescence/Multi-Detection

Table II. Primer sequences for RT-qPCR.

Gene name	Primer-forward (5'-3')	Primer-reverse (5'-3')
RHPN1-AS1	GCTCCTGGTCATCAAGTTCCTCT	GCACAGGCACCAGAATGATCC
TOP2A	AACGAGACCATGCCTCACC	CAAACCAGCCTCTTTCTTCG
β-actin	TCACCAACTGGGACGACATG	GTCACCGGAGTCCATCACGAT
miR-6884-5p	AGAGGCTGAGAAGGTGATGT	AGAGGCTGAGAAGGTGATGT
U6	CTCGCTTCGGCAGCACATATACTA	ACGAATTTGCGTGTCATCCTTGCG

Microplate Reader (BioTek) was used to detect luciferase activity.

RIP assay. Magna RIP RNA-binding protein immunoprecipitation kit (Millipore, USA) was used to perform RNA immunoprecipitation (RIP) assay. Cells transfected with miR-6884-5p mimic or negative control (NC) were lysed by RIP lysis buffer and incubated in RIP buffer containing magnetic beads supplemented with Anti-Ago2 or negative control (Anti-IgG). After incubation with Proteinase K and the immunoprecipitated RNA, the extracted RNAs isolated by TRIzol reagent (Invitrogen; Thermo Fisher Scientific, Inc.) were detected by RT-qPCR.

RNA pull-down assay. Pierce™ RNA 3' End Desthiobiotinylation Kit (Thermo Fisher Scientific, Inc.) was used to conduct RNA pull-down assay. In brief, first, biotin-labeled miR-6884-5p mimic (Bio-miR-6884-5p) or biotin-labeled miR-6884-5p NC (Bio-NC) was obtained from Guangzhou RiboBio Co., Ltd. After transfection, harvested cells were lysed and treated with an incubation of streptavidin magnetic beads, forming RNA-protein complexes, after which protein K and DNase A were added. RNA was separated from the complex and TOP2A mRNA expression was detected by RT-qPCR.

Western blot analysis. After transfection for 48 h, total proteins were extracted from cells by RIPA lysis buffer (Sigma; Merck KGaA) and qualified by BCA detection kit (Thermo Fisher Scientific, Inc.). After separating by 10% SDS-PAGE, proteins were transferred to PVDF membranes (Millipore, USA). After blocking by 5% skim milk powder for 1 h, the membranes were treated with the TOP2A antibody (anti-TOP2A, dilution 1:1,000, ab52934, Abcam) and β-actin antibody (rabbit anti-β-actin, dilution 1:1,000, ab8227, Abcam) at 4˚C for 12 h. Next day, the secondary antibody (goat anti-rabbit, dilution 1:10,000, ab6721, Abcam) was added into the membranes for 1 h. Protein bands were visualized via Immobilon Western Chemiluminescent HRP Substrate (Millipore), and the densitometry was analyzed using AlphaEase FC 6.0.2 (Alpha Innotech Corp.).

Statistical analysis. Our statistical analysis was performed by GraphPad Prism 8.0 (GraphPad Software, Inc.). The Student's t-test (two-tailed) was applied to assess the statistical significance between two groups, while the statistical significance among three or more groups was determined by one-way ANOVAs with Dunnett's multiple comparisons test. Correlation analysis in GraphPad Prism 8.0 was used to analyze the correlation among RHPN1-AS1, miR-6884-5p and *TOP2A* expression level. Data are presented as the mean ± standard deviation (SD). $P<0.05$ was regarded as statistically significant.

Results

The identification of genes of interest in this study. We firstly screened out the significantly upregulated genes from GSE119056 and GSE23392 data series downloaded from GEO database. There were 50 overlapped genes between the two datasets (Fig. 1A). The 50 genes then went through a STRING networking analysis at the highest confidence level 0.9. Among the 10 genes in the network, we noted that *TOP2A* (Fig. 1B) had been studied in ovarian cancer and was considered to be a tumor promoter; however, it had not been studied in a ceRNA network in ovarian cancer before. Thus, *TOP2A* was selected as the gene of interest in our study. According to the GEPIA database, *TOP2A* was found to be significantly upregulated in ovarian cancer as well (Fig. 1C). On the other hand, we have long paid attention to lncRNA RHPN1-AS1, and we noted that it was significantly upregulated in ovarian cancer (from GEPIA, Fig. 1D) and is considered to be a tumor promoter in ovarian cancer by working a ceRNA mechanism (29,30). There were two overlapped miRNAs between the target miRNAs of RHPN1-AS1 and the target miRNAs of *TOP2A*: miR-485-5p and miR-6884-5p (Fig. 1E). miR-485-5p has been extensively studied in ovarian cancer, whereas miR-6884-5p has been limitedly studied. Thus, we chose miR-6884-5p as our miRNA of interest. The RHPN1-AS1/miR-6884-5p/*TOP2A* interactome was then studied for the first time in our study.

RHPN1-AS1 distributed in the cytoplasm is upregulated in ovarian cancer. It was necessary to firstly understand the characteristic of RHPN1-AS1 in ovarian cancer. After eliminating the tissue samples with borderline type (n=12) and unknown type (n=3), we analyzed RHPN1-AS1 expression in 22 ovarian cancer tissues and 22 corresponding normal tissues by RT-qPCR. The expression of RHPN1-AS1 in the tumor tissues was nearly 2.7 times of that in the corresponding normal tissues (Fig. 2A). RT-qPCR was also applied to compare how RHPN1-AS1 was expressed in ovarian cancer cell lines (SKOV3, OVCAR3, CaoV3 and OV90) and a normal ovarian epithelial cell line (HOSE). The amount of RHPN1-AS1 expression in every ovarian cancer cell line was more than twice of that in normal ovarian epithelial cell line (Fig. 2B). In addition, SKOV3 and OVCAR3 cells displayed the highest RHPN1-AS1 expression, triple higher than that in the HOSE cells. Thus, SKOV3 and OVCAR3 cells were chosen for further

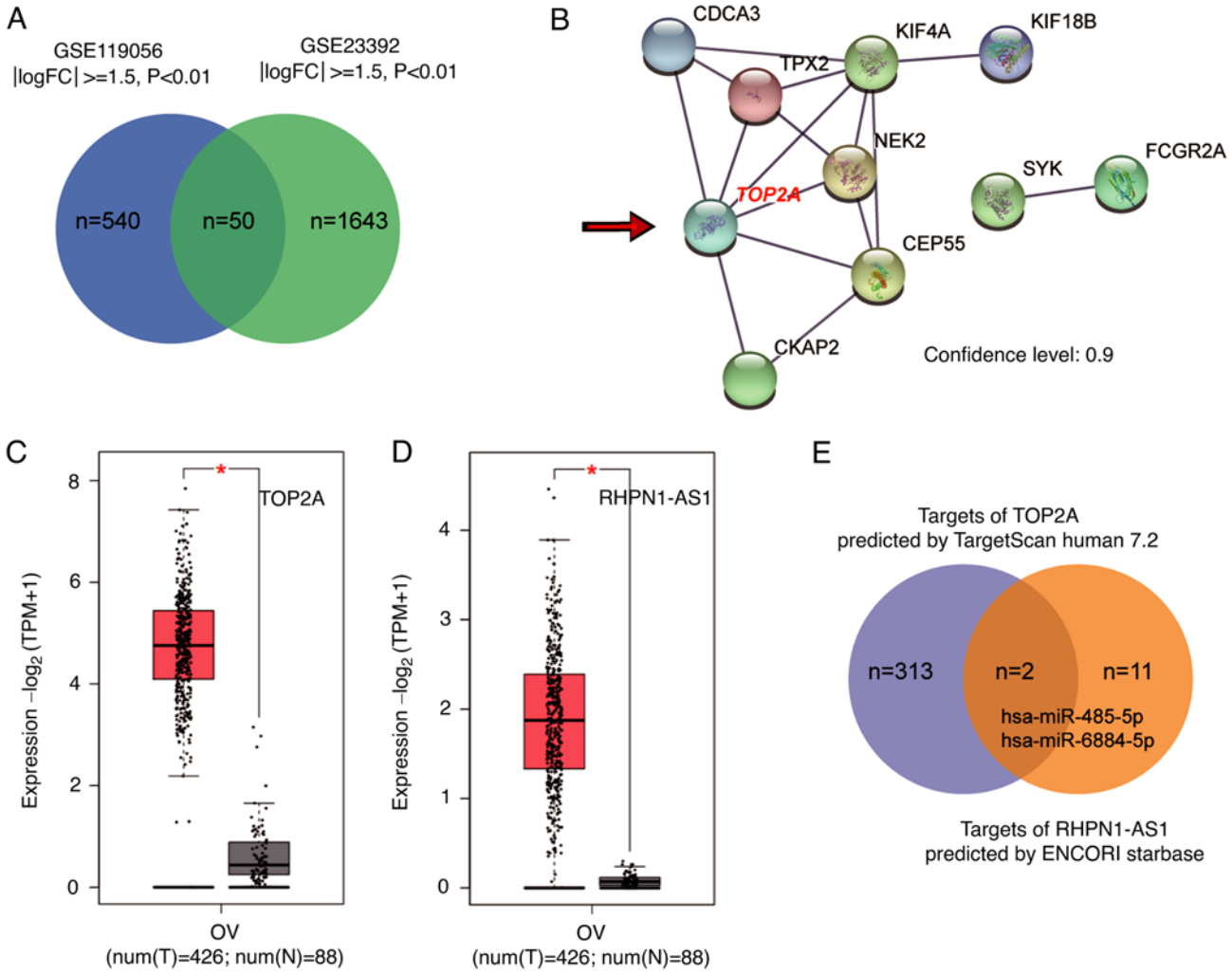

Figure 1. Identification of genes of interest in this study. (A) Overlapping genes of the significantly upregulated genes from GSE119056 and GSE23392 data series downloaded from from Gene Expression Omnibus (GEO) database. FC, fold change. (B) STRING analysis of the overlapping genes from A. The confidence level was set at 0.9. (C) Expression of *TOP2A* in ovarian cancer using the Gene Expression Profiling Interactive Analysis (GEPIA) database. OV, ovarian cancer; T, tumor; N, normal. (D) Expression of RHPN1-AS1 in ovarian cancer using GEPIA database. OV, ovarian cancer; T, tumor; N, normal. *P<0.01. (E) Overlapping miRNAs between the targets of *TOP2A* predicted by TargetScan Human 7.2 and the targets of RHPN1-AS1 predicted by ENCORI Starbase database. *TOP2A*, DNA topoisomerase IIα; RHPN1-AS1, Rhophilin Rho GTPase binding protein 1 antisense RNA1.

cellular behavioral experiments. Subsequently, we researched the intracellular distribution of RHPN1-AS1. RHPN1-AS1 was mainly distributed in the cell cytoplasm (Fig. 2C). At the same time, the FISH assay further verified that the distribution of RHPN1-AS was in the cell cytoplasm (Fig. 2D).

Silencing of RHPN1-AS1 suppresses ovarian cancer progression. Before the ovarian cancer cellular behavioral experiments, the transfection efficiency of the RHPN1-AS1 silencing plasmids (si-lnc) was detected by RT-qPCR. si-lnc was able to downregulate RHPN1-AS1 expression compared to the blank control group (Fig. S1A). After transfection with si-lnc for 72 h, the cell viability was significantly decreased especially in SKOV3 and OVCAR3 cells (Fig. S1B). Then, the cellular behavioral experiments were performed in SKOV3 and OVCAR3 cells. BrdU assay revealed that knockdown of RHPN1-AS1 obviously repressed cell proliferation by approximately 40% compared to the blank control group in the OVCAR3 and SKOV3 cells (Fig. 3A). MTT assay showed silencing of RHPN1-AS1 significantly impaired the cell viability of the OVCAR3 and SKOV3 cells (Fig. 3B). Colony formation assay revealed that knockdown of RHPN1-AS1 reduced the number of colonies by 35% in the SKOV3 cells and 60% in OVCAR3 cells (Fig. 3C). Cell adhesion assay demonstrated si-lnc suppressed cell adhesion by approximately 30% compared to the blank control group (Fig. 3D). Caspase-3 activity assay demonstrated that the silencing of RHPN1-AS1 increased cell apoptosis to over twice the level as the blank control group (Fig. 3E). Moreover, flow cytometry was similar to the results of the caspase-3 activity assay, which showed that the apoptosis rate of the si-lnc group was increased by more than 2 times compared with the blank group (Fig. 3F). Additionally, wound healing assay demonstrated that the silencing of RHPN1-AS1 induced inhibition of cell migration (Fig. 3G). These data suggest that silencing of RHPN1-AS1 functionally impedes ovarian cancer progression *in vitro*.

RHPN1-AS1 is able to sponge miR-6884-5p in ovarian cancer. ENCORI starbase algorithm (http://starbase.sysu.edu.cn/) was employed for the exploration of potential targets

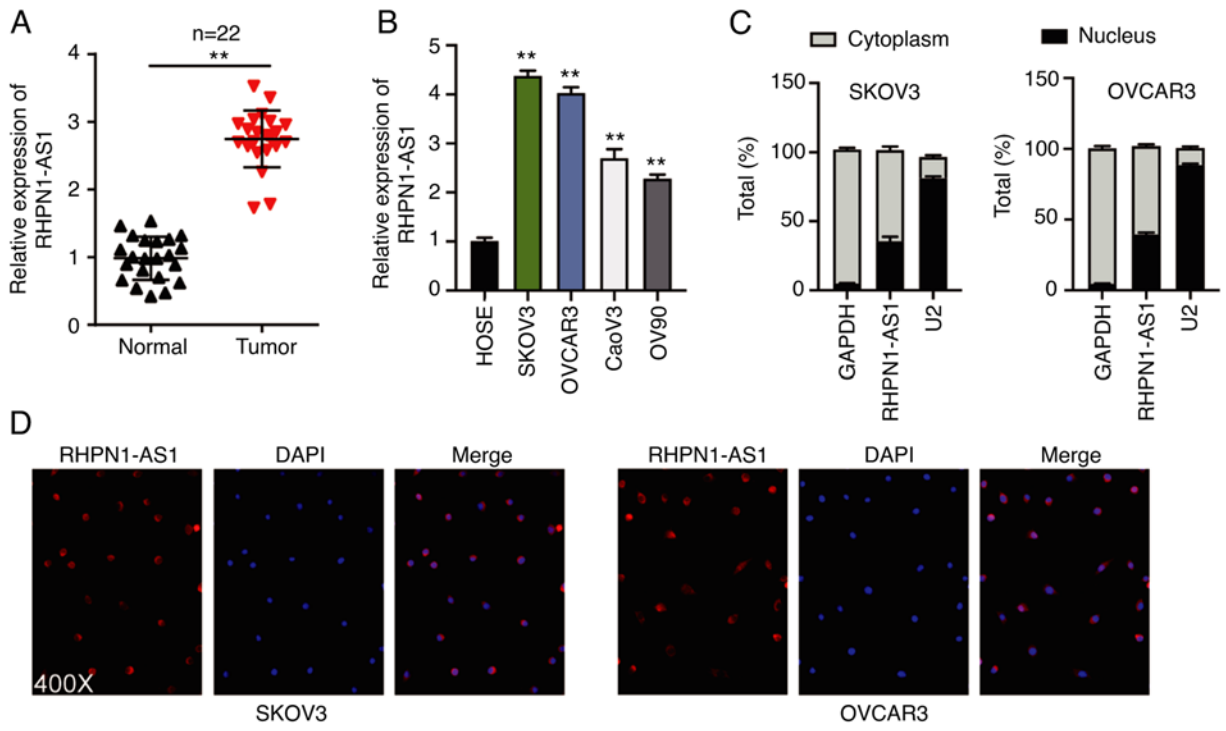

Figure 2. Expression and distribution of RHPN1-AS1 in ovarian cancer. (A) Expression of RHPN1-AS1 in ovarian cancer tissues and corresponding normal tissues. **P<0.001 compared with normal tissues. (B) Expression of RHPN1-AS1 in ovarian cancer cell lines (SKOV3, OVCAR3, CaOV3 and OV90) and normal ovarian epithelial cell (HOSE). **P<0.001 compared with HOSE cells. (C) Cytoplasmic/nuclear fractionation assay determined the intracellular distribution of RHPN1-AS1 in SKOV3 and OVCAR3 cells. (D) FISH assay was used to determine the location of RHPN1-AS1 in SKOV3 and OVCAR3 cells. Data are presented as mean ± SD. RHPN1-AS1, Rhophilin Rho GTPase binding protein 1 antisense RNA1.

for RHPN1-AS1 in ovarian cancer. As a result, miR-6884-5p is a target of RHPN1-AS1, and the potential binding site between RHPN1-AS1 and miR-6884-5p is shown in Fig. 4A. Compared to the mimic NC group, the luciferase activity was significantly reduced by about 50% only in cells that were co-transfected with the miR-6884-5p mimic and RHPN1-AS1-WT plasmids (Fig. 4B). RIP assay confirmed that RHPN1-AS1 binding to miR-6884-5p was dramatically pulled down by anti-Ago2 antibody (Fig. 4C). After eliminating the tissue samples with borderline type (n=12) and unknown type (n=3), miR-6884-5p expression in ovarian cancer tissues was 50% lower than that observed in the corresponding normal tissues (Fig. 4D). The correlation analysis displayed an inverse correlation between miR-6884-5p and RHPN1-AS1 expression (Fig. 4E). Moreover, in Fig. 4F, miR-6884-5p exhibited a lower expression in ovarian cancer SKOV3 and OVCAR3 cells than that noted in the normal ovarian HOSE cells, showing that miR-6884-5p expression in ovarian cancer cells were only approximately 55% of that in HOSE cells. As expected, silencing of RHPN1-AS1 positively regulated miR-6884-5p expression, increasing it by more than 3-fold compared to the blank control group (Fig. 4G). These findings strongly confirmed RHPN1-AS1 sponges miR-6884-5p in ovarian cancer.

Silencing of RHPN1-AS1 suppresses ovarian cancer progression in vitro via an miR-6884-5p-dependent mechanism. Further, rescue experiments were performed to ascertain whether RHPN1-AS1 facilitates ovarian cancer progression via miR-6884-5p. As a result, compared to the blank control group, si-RHPN1-AS1 increased miR-6884-5p expression by twice while decreasing RHPN1-AS1 expression by 75%, and the miR-6884-5p inhibitor decreased miR-6884-5p expression by 70% while it had no effect on RHPN1-AS1 expression (Fig. 5A). In addition, miR-6884-5p inhibitor + si-RHPN1-AS1 did not change miR-6884-5p expression while this co-transfection suppressed RHPN1-AS1 expression by 70% compared to the blank control group (Fig. 5A). In BrdU assay, compared to the blank control group, silencing of RHPN1-AS1 repressed cell proliferation by 30 to 40% while the miR-6884-5p inhibitor promoted cell proliferation by 40%, which was restored in the co-transfection group (Fig. 5B). MTT assay revealed that the miR-6884-5p inhibitor exerted an oncogenic effect on cell viability, and the oncogenic effect induced by the miR-6884-5p inhibitor was abrogated by the silencing of RHPN1-AS1 (Fig. 5C). Colony formation assay showed that the downregulation of miR-6884-5p increased the number of cell colonies compared to the blank group, but this effect was reversed by silencing of RHPN1-AS1 (Fig. 5D). Cell adhesion assay demonstrated that the silencing of RHPN1-AS1 decreased cell adhesion by 30%, while the miR-6884-5p inhibitor promoted it by about 40% compared to the blank control group, and these effects were restored by the miR-6884-5p inhibitor + si-RHPN1-AS1 (Fig. 6A). The result of caspase-3 activity assay demonstrated that the silencing of RHPN1-AS1 increased cell apoptosis to a level twice that of the blank control, while the miR-6884-5p inhibitor suppressed it by about 40% compared to the blank control group, and these effects were restored by the miR-6884-5p inhibitor + si-RHPN1-AS1 (Fig. 6B). The result

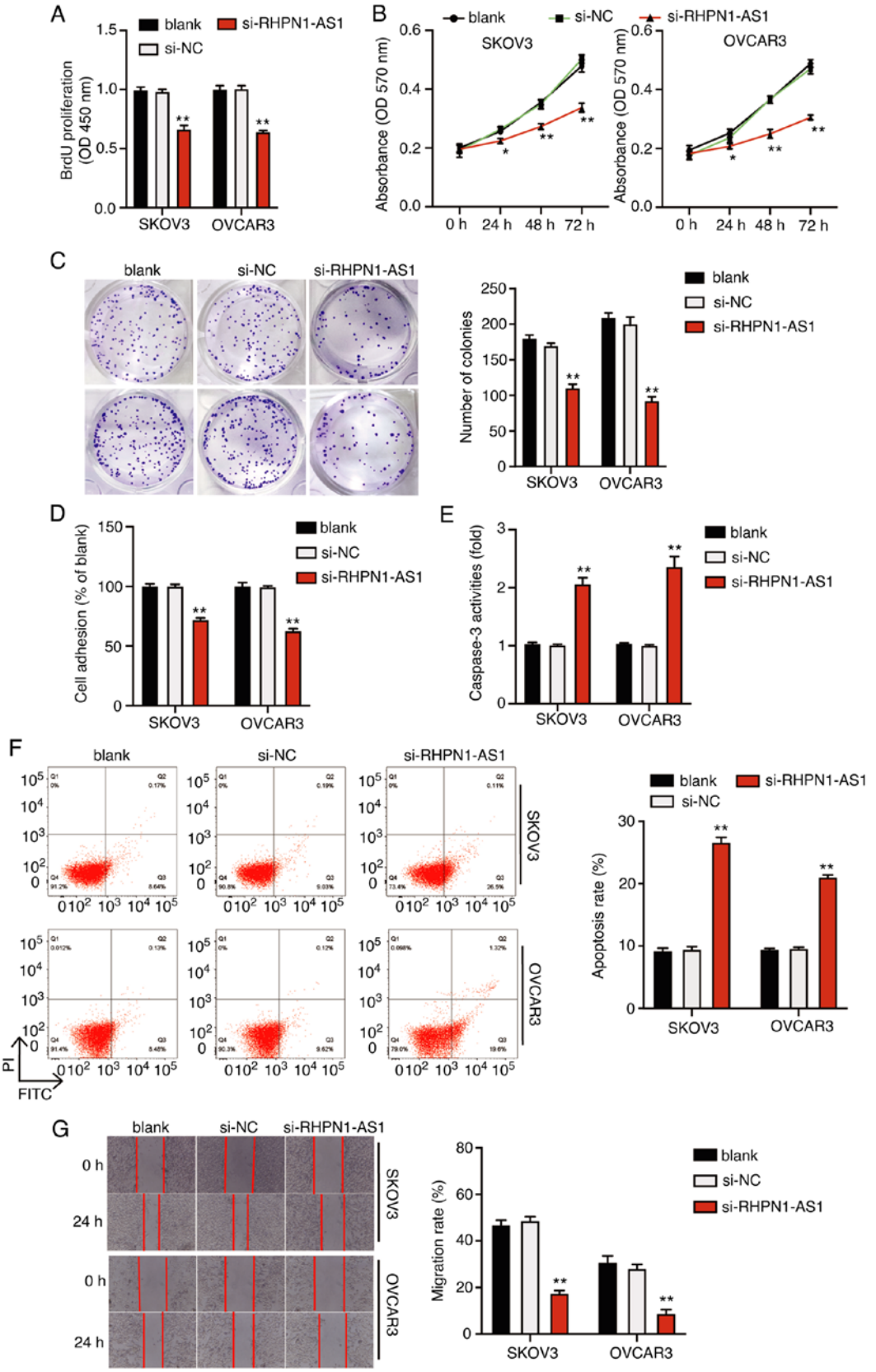

Figure 3. Silencing of RHPN1-AS1 suppresses ovarian cancer progression. (A) BrdU incorporation assay was used to demonstrate cell proliferation of SKOV3 and OVCAR3 cells transfected with RHPN1-AS1 silencing plasmids. (B) MTT assay was applied to evaluate cell viability of SKOV3 and OVCAR3 cells transfected with RHPN1-AS1 silencing plasmids. (C) Colony formation assay was performed to determine the number of colonies of SKOV3 and OVCAR3 cells transfected with RHPN1-AS1 silencing plasmids. (D) Cell adhesion assay was applied to evaluate cell adhesion of SKOV3 and OVCAR3 cells transfected with RHPN1-AS1 silencing plasmids. (E) Caspase-3 activity assay was performed to determine cell apoptosis of SKOV3 and OVCAR3 cells transfected with RHPN1-AS1 silencing plasmids. (F) Flow cytometry assay was carried out to determine cell apoptosis of SKOV3 and OVCAR3 cells transfected with RHPN1-AS1 silencing plasmids. (G) Wound healing assay was used to measure cell migration ability of SKOV3 and OVCAR3 cells transfected with RHPN1-AS1 silencing plasmids. *P<0.05, **P<0.001 compared with the blank control group; blank, blank control. Data are presented as mean ± SD. RHPN1-AS1, Rhophilin Rho GTPase binding protein 1 antisense RNA1.

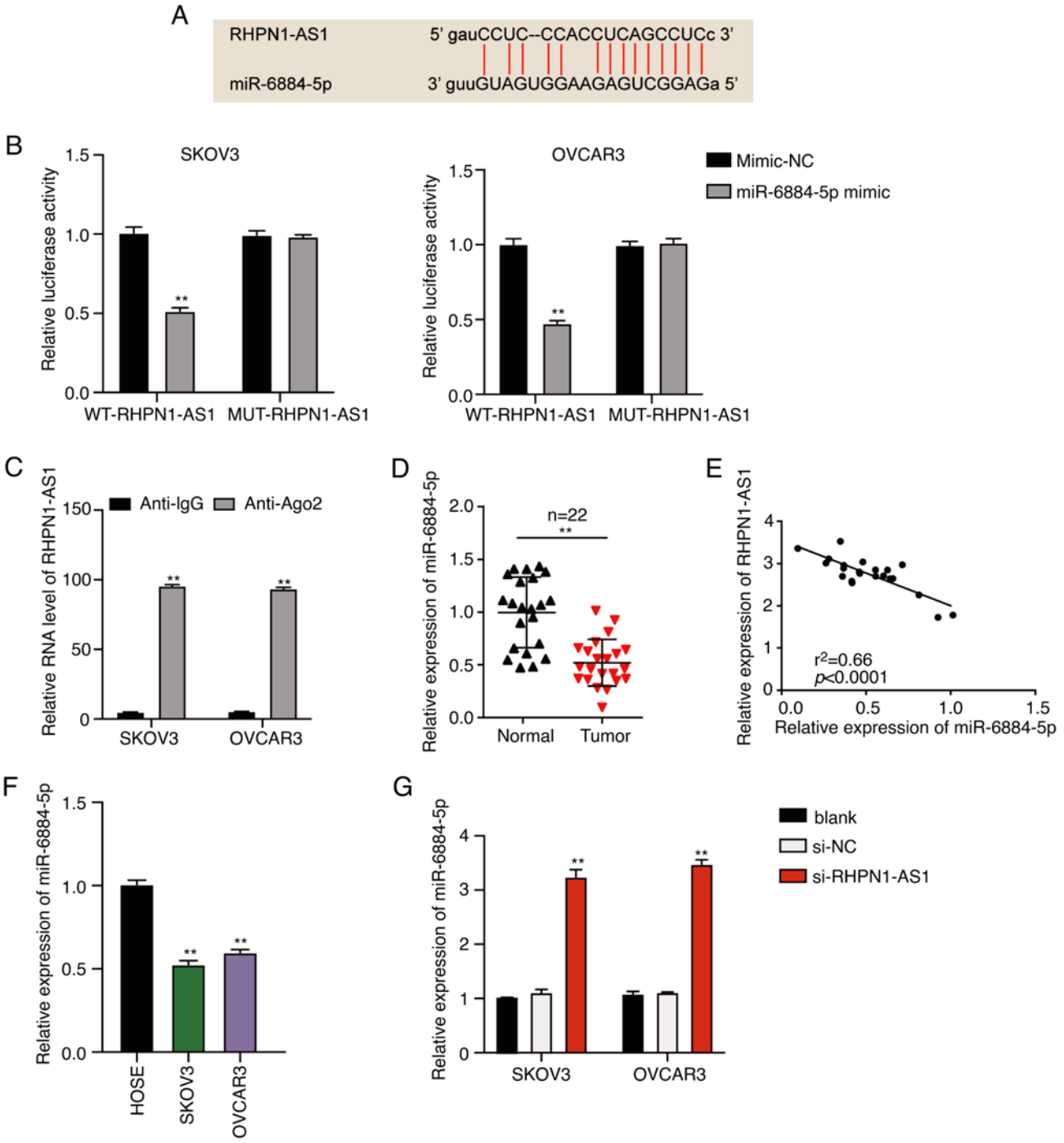

Figure 4. RHPN1-AS1 serves as a sponge for miR-6884-5p. (A) The potential binding site between RHPN1-AS1 and miR-6884-5p was predicted by ENCORI Starbase algorithm. (B) Dual-luciferase reporter assay in SKOV3 and OVCAR3 cells transfected with miR-6884-5p mimic and RHPN1-AS1-WT or RHPN1-AS1-MUT reporter plasmids. **P<0.001 compared with mimic-NC. (C) RIP analysis showed that RHPN1-AS1 was abundantly pulled down when transfected with the miR-6884-5p mimic in the SKOV3 and OVCAR3 cells. **P<0.001 compared to anti-IgG. (D) Expression of miR-6884-5p in ovarian cancer and normal tissues. **P<0.001 compared with normal tissues. (E) A negative correlation between RHPN1-AS1 and miR-6884-5p expression in tumorous tissues was confirmed by correlation analysis. (F) Expression of miR-6884-5p in SKOV3 and OVCAR3 cells. **P<0.001 compared with HOSE cells. (G) Silencing of RHPN1-AS1 significantly upregulated the expression of miR-6884-5p in SKOV3 and OVCAR3 cells. **P<0.001 compared with the blank control group. blank, blank control. Data are presented as mean ± SD. RHPN1-AS1, Rhophilin Rho GTPase binding protein 1 antisense RNA1.

of the flow cytometric assay showed that downregulation of miR-6884-5p inhibited cell apoptosis, while miR-6884-5p inhibitor eliminated the pro-apoptotic effect of the silencing of RHPN1-AS1 (Fig. 6C). In addition, wound healing assay confirmed that the silencing of RHPN1-AS1 attenuated the promotion of migration in response to miR-6884-5p inhibition (Fig. 6D). Thereby, our results suggest that RHPN1-AS1 promotes ovarian cancer progression via a miR-6884-5p-dependent mechanism.

miR-6884-5p sponged by RHPN1-AS1 could target TOP2A in ovarian cancer. TargetScan was applied to predict targets for miR-6884-5p. *TOP2A* might be the most suitable target. The sequence of *TOP2A* mRNA that contains miR-6884-5p's binding

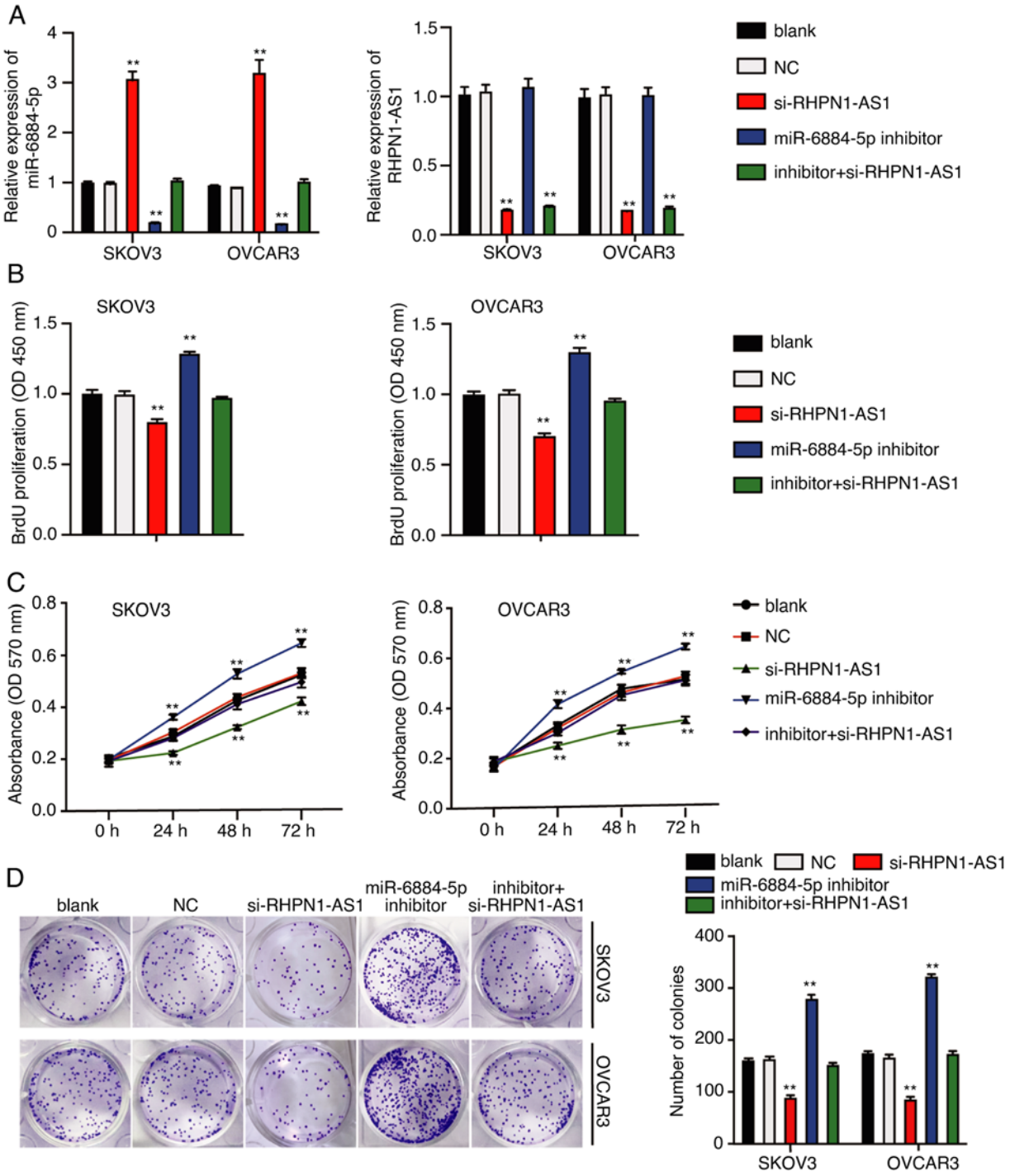

Figure 5. Silencing of RHPN1-AS1 suppresses viability and proliferation of ovarian cancer cells *in vitro* via a miR-6884-5p-dependent mechanism. (A) The transfection efficiencies of the silencing of RHPN1-AS1 and the miR-6884-5p inhibitor in SKOV3 and OVCAR3 cells were determined by RT-qPCR. (B) niR-6884-5p inhibitor facilitated cell proliferation ability of SKOV3 and OVCAR3 cells. The introduction of RHPN1-AS1 silencing plasmids reversed the oncogenic effect of miR-6884-5p inhibitor on cell proliferation. (C) miR-6884-5p inhibitor promoted cell viability of SKOV3 and OVCAR3 cells. The introduction of the silencing of RHPN1-AS1 abrogated the oncogenic effect of the miR-6884-5p inhibitor on cell viability. (D) miR-6884-5p inhibitor promoted the colony information of SKOV3 and OVCAR3 cells. RHPN1-AS1 knockdown reversed the oncogenic effect of the miR-6884-5p inhibitor on cell colony formation ability. Data are presented as mean ± SD. **P<0.001 compared with the blank control group. blank, blank control; NC, negative control; inhibitor, miR-6884-5p inhibitor. RHPN1-AS1, Rhophilin Rho GTPase binding protein 1 antisense RNA1.

site is shown in Fig. 7A. Dual-luciferase reporter assay demonstrated that the luciferase activity of SKOV3 and OVCAR3 cells transfected with TOP2A-WT was obviously decreased by the introduction of the miR-6884-5p mimic by about 50% compared to the mimic NC (Fig. 7B). RNA pull-down assay revealed that *TOP2A* was significantly pulled down by bio-miR-6884-5p (Fig. 7C). After eliminating the tissue samples with borderline type (n=12) and unknown type (n=3), *TOP2A* expression in invasive ovarian cancer tissues was more than twice that noted in the corresponding normal tissues (Fig. 7D). Moreover, *TOP2A* expression exhibited a negative correlation with miR-6884-5p expression (Fig. 7E). Following analysis of RT-qPCR, *TOP2A*

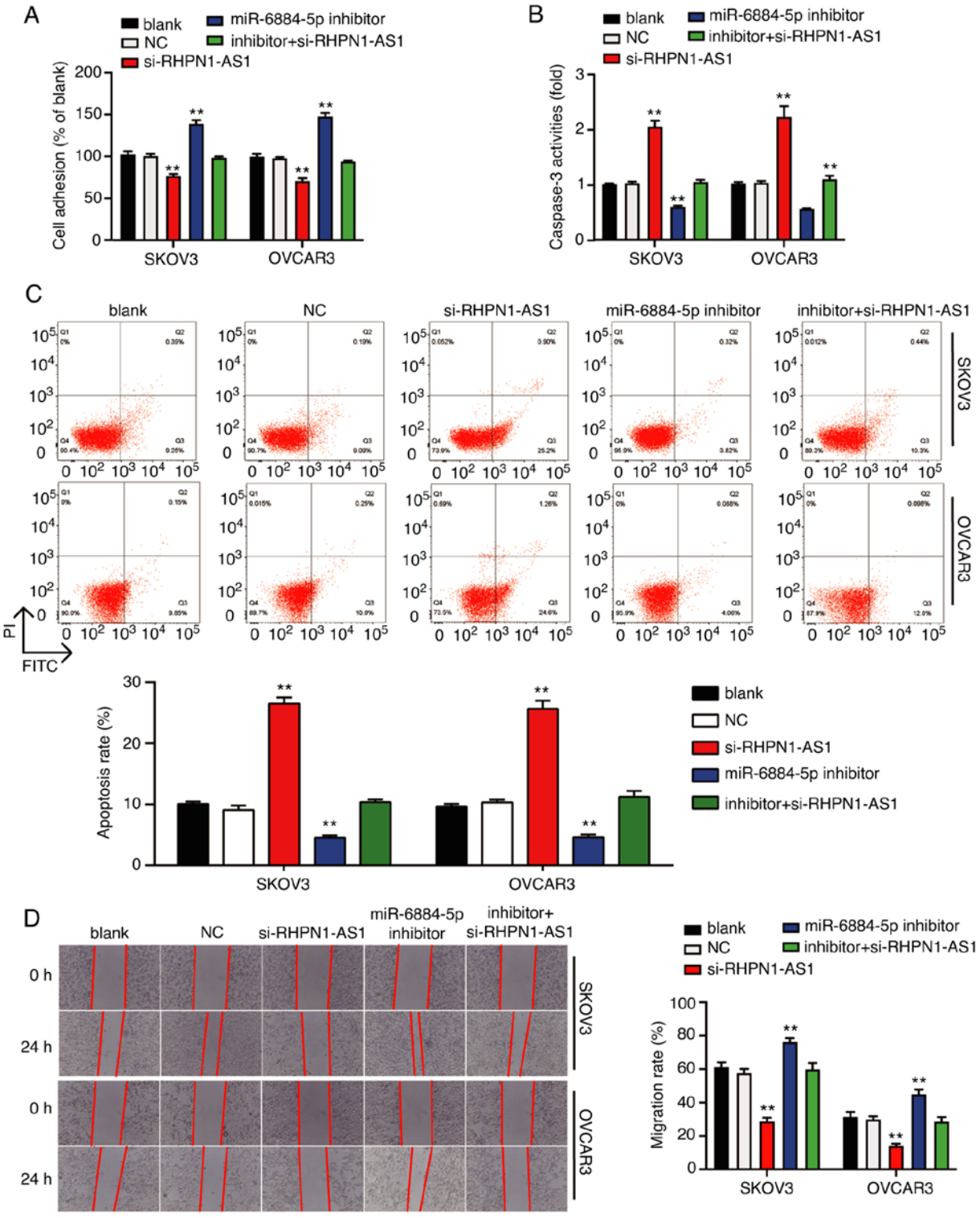

Figure 6. Silencing of RHPN1-AS1 promotes apoptosis and suppresses migration of ovarian cancer cells via a miR-6884-5p-dependent mechanism. (A) miR-6884-5p inhibitor promoted cell adhesion of SKOV3 and OVCAR3 cells. The introduction of the silencing of RHPN1-AS1 abrogated the oncogenic effect of miR-6884-5p inhibitor on cell adhesion. (B) miR-6884-5p inhibitor reduced the caspase-3 activity of SKOV3 and OVCAR3 cells. The knockdown of RHPN1-AS1 restored the inhibition of the caspase-3 activity induced by miR-6884-5p inhibitor. (C) miR-6884-5p inhibitor decreased cell apoptosis of SKOV3 and OVCAR3 cells. Downregulation of RHPN1-AS1 reversed the inhibition of cell apoptosis induced by miR-6884-5p inhibitor. (D) miR-6884-5p inhibitor promoted cell migration ability of SKOV3 and OVCAR3 cells. The knockdown of RHPN1-AS1 reversed the oncogenic effect of the miR-6884-5p inhibitor on cell migration. Data are presented as mean ± SD. **P<0.001 compared with the blank control group. blank, blank control; NC, negative control; inhibitor, miR-6884-5p inhibitor. RHPN1-AS1, Rhophilin Rho GTPase binding protein 1 antisense RNA1.

was obviously highly expressed in ovarian cancer SKOV3 and OVCAR3 cells than that noted in the HOSE cells (Fig. 7F). The miR-6884-5p inhibitor was identified to promote *TOP2A* mRNA expression by 80% compared to the blank control group (Fig. 7G). The western blot assay further confirmed that the miR-6884-5p inhibitor enhanced the TOP2A protein expression by 1.3-fold, as

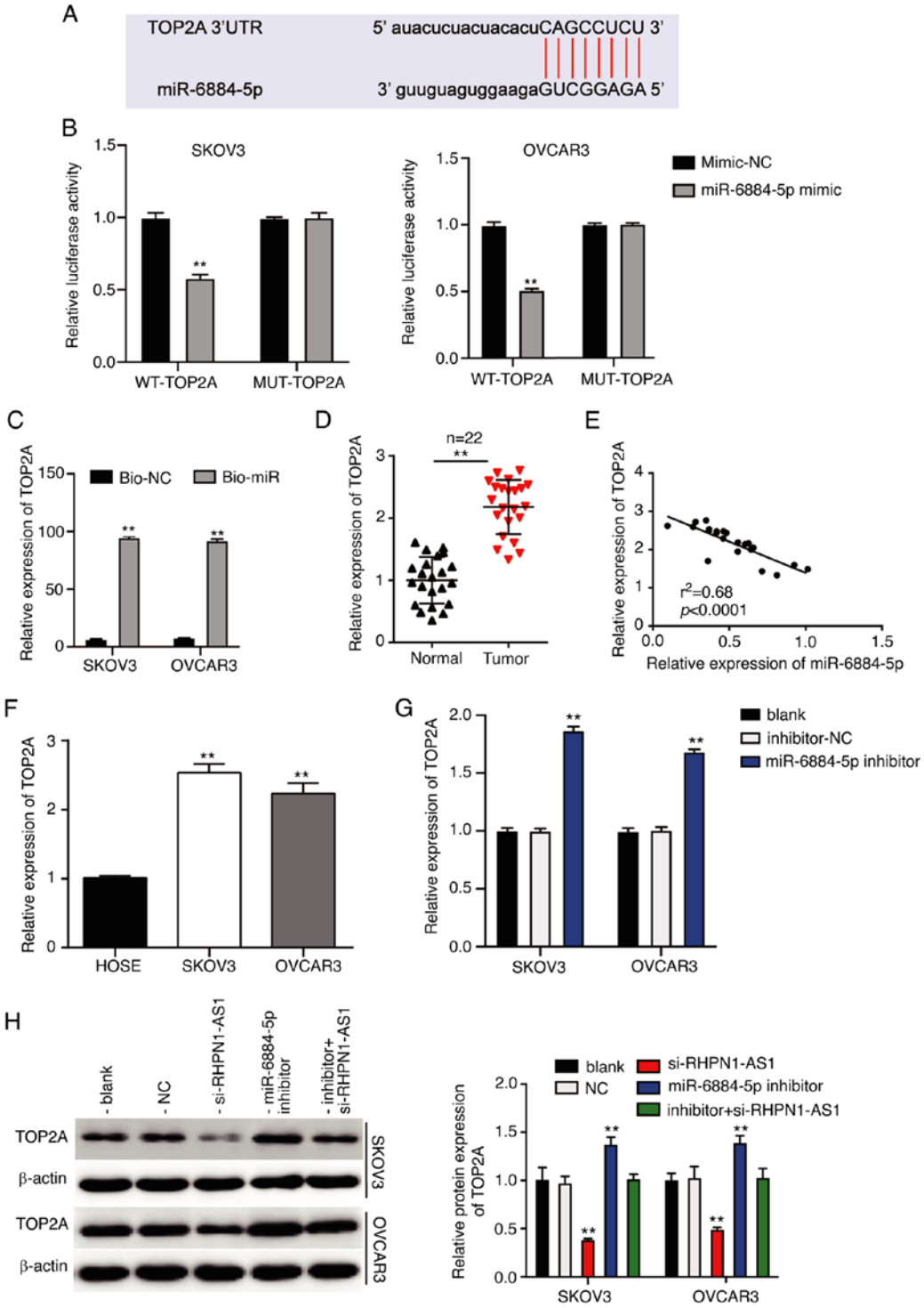

Figure 7. miR-6884-5p directly targets *TOP2A* in ovarian cancer cells. (A) The sequence of *TOP2A* containing the miR-6884-5p binding site. (B) Luciferase activity in SKOV3 and OVCAR3 cells that were co-transfected with the miR-6884-5p mimic and wild-type (WT) or mutant type (MUT) of *TOP2A* 3'-UTR luciferase reporter plasmids was detected. **P<0.001 compared with the mimic-NC. (C) RNA pull-down analysis showed that *TOP2A* was abundantly pulled down when transfected with Bio-miR-6884-5p mimic in SKOV3 and OVCAR3 cells. Bio-miR, biotin-labeled miR-6884-5p mimic; Bio-NC, biotin-labeled negative control. **P<0.001 compared to Bio-NC. (D) Expression of *TOP2A* in ovarian cancer tissues and corresponding normal tissues. **P<0.001 compared with the normal tissues. (E) Significant inverse correlation between miR-6884-5p and *TOP2A* expression in tumor tissues was determined by correlation analysis. (F) mRNA expression of *TOP2A* in ovarian cancer SKOV3 and OVCAR3 cells. **P<0.001 compared with HOSE cells. (G) miR-6884-5p inhibitor promoted mRNA expression of *TOP2A* in SKOV3 and OVCAR3 cells. **P<0.001 compared with the blank control group. (H) Effect of the silencing of RHPN1-AS1 and miR-6884-5p on TOP2A protein expression was detected by western blot analysis. blank, blank control; NC, negative control; inhibitor, miR-6884-5p inhibitor. **P<0.001 compared with the blank control group. Data are presented as mean ± SD. *TOP2A*, DNA topoisomerase IIα.

well as the silencing of RHPN1-AS1 led to a decrease in TOP2A protein expression (Fig. 7H). Therefore, miR-6884-5p targets *TOP2A* in ovarian cancer, which is regulated by RHPN1-AS1.

miR-6884-5p negatively regulates TOP2A in ovarian cancer. To explore the effect of the miR-6884-5p/*TOP2A* axis in ovarian cancer, *TOP2A* siRNA was used to transfect ovarian

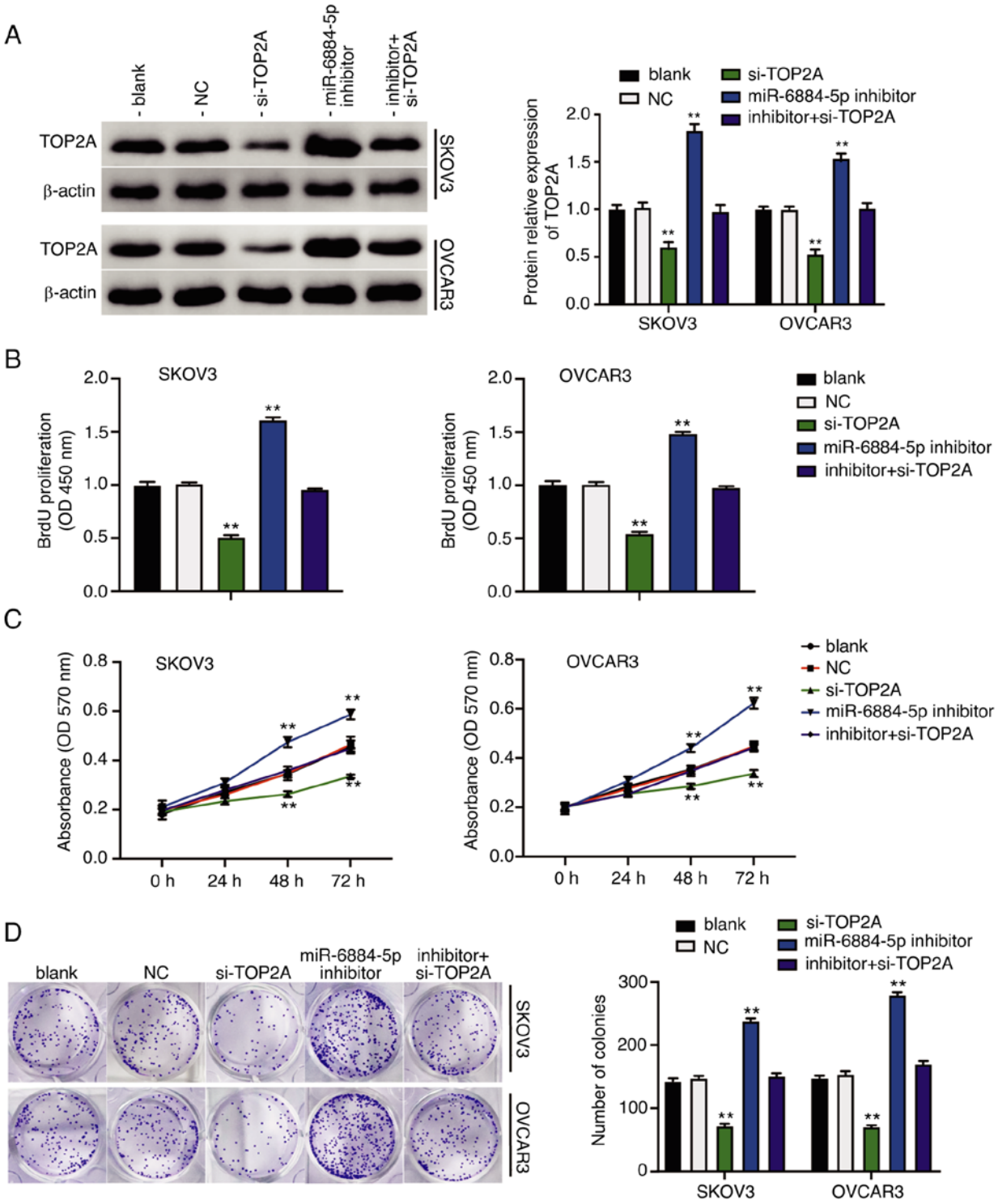

Figure 8. miR-6884-5p negatively regulates *TOP2A* and affects the viability and proliferation of ovarian cancer cells. (A) The transfection efficiencies of *TOP2A* siRNA and miR-6884-5p inhibitor in SKOV3 and OVCAR3 cells were determined by western blot analysis. (B) BrdU assay demonstrated that the decreased cell proliferation of SKOV3 and OVCAR3 cells transfected with *TOP2A* siRNA was reversed when co-transfected with miR-6884-5p inhibitor. (C) MTT assay indicated that the decreased cell viability of SKOV3 and OVCAR3 cells transfected with *TOP2A* siRNA was reversed when co-transfected with miR-6884-5p inhibitor. (D) Colony formation assay indicated that the reduced cell colony number of SKOV3 and OVCAR3 cells transfected with *TOP2A* siRNA was reversed when co-transfected with the miR-6884-5p inhibitor. Data are present as mean ± SD. **P<0.001 compared with the blank control group. blank, blank control; NC, negative control; inhibitor, miR-6884-5p inhibitor; TOP2A, DNA topoisomerase IIα.

cancer cells. As expected, silencing of *TOP2A* dramatically inhibited TOP2A protein expression compared to the blank control group (Figs. 8A and S2); at the same time, miR-6884-5p inhibitor restored the effect of the silencing of RHPN1-AS1 (Fig. 8A). As determined by the BrdU assay, silencing of *TOP2A* in SKOV3 and OVCAR3 cells caused about 50% inhibition in cell viability compared to the blank control group, which was restored by miR-6884-5p inhibitor + *TOP2A* siRNA (Fig. 8B). According to the MTT assay, silencing of *TOP2A* led to inhibition of cell viability, which was restored

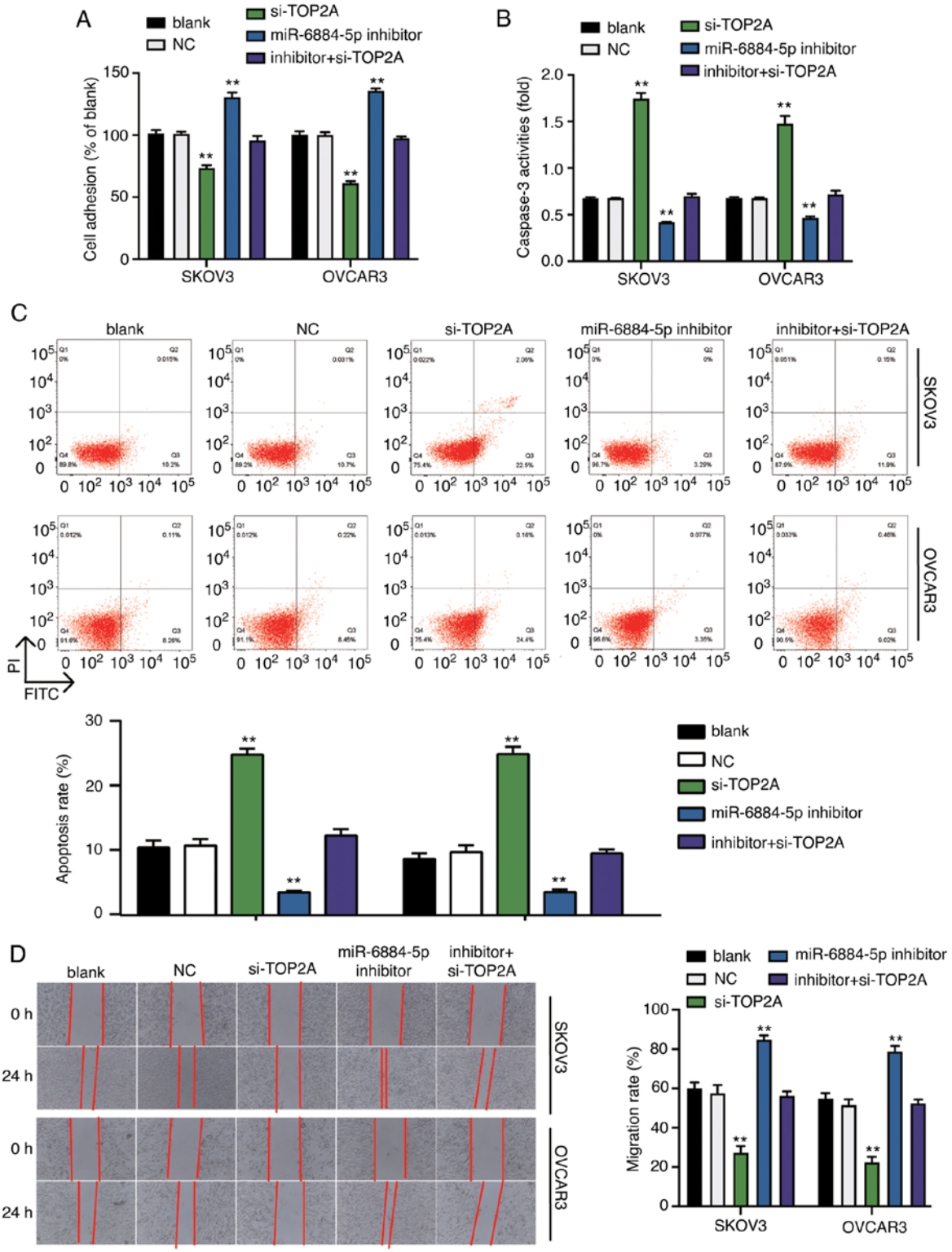

Figure 9. miR-6884-5p negatively regulates *TOP2A* and affects the apoptosis and migration of ovarian cancer cells. (A) *TOP2A* siRNA inhibited cell adhesion of SKOV3 and OVCAR3 cells. The introduction of miR-6884-5p inhibitor abrogated this effect. (B) Caspase-3 activity assay revealed that the increased cell apoptosis of SKOV3 and OVCAR3 cells transfected with *TOP2A* siRNA was reversed when co-transfected with the miR-6884-5p inhibitor. (C) Flow cytometric assay revealed that the increased cell apoptosis of SKOV3 and OVCAR3 cells transfected with *TOP2A* siRNA was reversed when co-transfected with miR-6884-5p inhibitor. (D) Wound healing assay showed that the decrease in cell migration ability of SKOV3 and OVCAR3 cells transfected with *TOP2A* siRNA was reversed when co-transfected with miR-6884-5p inhibitor. Data are presented as mean ± SD. **P<0.001 compared with the blank control group. blank, blank control; NC, negative control; inhibitor, miR-6884-5p inhibitor; *TOP2A*, DNA topoisomerase IIα.

by miR-6884-5p inhibitor + *TOP2A* siRNA (Fig. 8C). Colony formation assay showed that interference with *TOP2A* reduced the colony number to approximately 50% of the blank group, while miR-6884-5p inhibitor reversed the influence of *TOP2A* siRNA on the number of cell colonies (Fig. 8D). Cell adhesion assay demonstrated that silencing of *TOP2A* decreased

cell adhesion by 30% compared to the blank control group, and the decrease was restored by the miR-6884-5p inhibitor + *TOP2A* siRNA (Fig. 9A). Caspase-3 activity assay revealed that the miR-6884-5p inhibitor abolished the increase (more than 1.5 times compared to the blank control group) of cell apoptosis induced by silencing if *TOP2A* in the SKOV3 and OVCAR3 cells (Fig. 9B). The result of the flow cytometry assay showed that knockdown of *TOP2A* promoted cell apoptosis, while the miR-6884-5p inhibitor eliminated the apoptosis-promoting effect caused by the silencing of *TOP2A* (Fig. 9C). As for wound healing assay, silencing of *TOP2A* obviously suppressed the ability of cell migration, while the miR-6884-5p inhibitor abrogated the suppressive effect on cell migration modulated by the silencing of *TOP2A* (Fig. 9D). Herein, miR-6884-5p inhibition functionally decreased cell apoptosis and increased cell proliferation, viability and migration in ovarian tumor by releasing *TOP2A*. These lines of evidence confirm our hypothesis that RHPN1-AS1 promotes ovarian carcinogenesis through sponging miR-6884-5p and releasing *TOP2A*.

Discussion

In the present study, we identified that the upregulation of Rhophilin Rho GTPase binding protein 1 antisense RNA1 (RHPN1-AS1) in ovarian cancer tissues and cell lines was closely correlated with cancer malignant behavior. Further research demonstrated that RHPN1-AS1 effectively suppressed miR-6884-5p which negatively regulated DNA topoisomerase IIα (*TOP2A*) in ovarian cancer. According to our rescue experiments, RHPN1-AS1 released *TOP2A* to reduce cell apoptosis and increase cell proliferation, viability, adhesion as well as migration via suppression of miR-6884-5p.

To date, due to the advent of next generation sequencing, mounting long noncoding RNAs (lncRNAs) have demonstrated regulatory effects in a variety of human tumors, including ovarian cancer. For instance, lnc-OC1 was found to suppress miR-34a and miR-34c to increase ovarian cancer cell proliferation and migration (31). lnc-PVT1 was found to exert aggressive properties in ovarian cancer by releasing SOX2 (32). On the contrary, there are few lncRNAs that act as suppressors in ovarian cancer, such as lnc-LAMC2-1:1 which could sponge miR-128-3p to induce cell apoptosis in ovarian cancer (33). As for RHPN1-AS1, its oncogenic role was confirmed in several human cancers. Specifically, upregulation of RHPN1-AS1 facilitated breast cancer progression by activating epithelial-mesenchymal transition (EMT) (15). Cell proliferation and migration abilities of cervical cancer could be effectively enhanced by the RHPN1-AS1/miR-299-3p/FGF2 axis (11). Upregulation of RHPN1-AS1 was found to promote gastric cancer by inhibiting miR-1299 and releasing ETS1 (12). In colorectal cancer, RHPN1-AS1 was identified to functionally modulate miR-7-5p by enhancing cell proliferation and migration (14). These previous studies strongly implicated an oncogenic role of RHPN1-AS1 across a wide spectrum of human cancers, although the study of whether RHPN1-AS1 is oncogenic in ovarian cancer remains limited. Herein, we designed a series of functional verifications to investigate how RHPN1-AS1 acts in ovarian cancer progression. We first ascertained whether RHPN1-AS1 was differentially expressed between tumor tissues and corresponding normal tissues. As a result, upregulation of RHPN1-AS1 was displayed in ovarian cancer tissues and cell lines, indicating an oncogenic role of RHPN1-AS1 in ovarian cancer. When we made further investigation, we found that the depletion of RHPN1-AS1 obviously induced cell apoptosis and impaired cell proliferation, viability, adhesion and migration of ovarian cancer cell lines. These findings revealed that RHPN1-AS1 was a promotional factor in ovarian cancer, in keeping with the previously mentioned studies which also indicated an oncogenic role of RHPN1-AS1.

Based on what was discussed earlier, RHPN1-AS1 exerts a regulatory function through sponging different miRNAs in diverse human tumors. Similarly, in our research, RHPN1-AS1 was identified to sponge miR-6884-5p in ovarian cancer. Interestingly, RHPN1-AS1 was also found to lead to the suppression of miR-6884-5p in breast cancer, and its downstream effector, ANXA11, was released to play an oncogenic role in cancer cell viability, apoptosis and migration (22). In addition, miR-6884-5p was reported to inhibit S100A16, which facilitated gastric cancer cell proliferation and invasion (22). In the present study, miR-6884-5p was revealed to be an ovarian cancer suppressor for the first time. Silencing of RHPN1-AS1 reversed the malignancy-promoting function of the miR-6884-5p inhibitor in ovarian cancer. Our results demonstrated that RHPN1-AS1 reduced cell apoptosis and strengthened cell proliferation, viability, adhesion and migration capability of ovarian cancer cell via the suppression of miR-6884-5p.

Similarly, we confirmed *TOP2A* to be a target mRNA for miR-6884-5p in ovarian cancer. According to diverse human cancer cellular behavioral experiments, *TOP2A* was reported to encode an enzyme that plays a role in DNA replication, transcription and controlling (34). To date, the research concerning the effects of *TOP2A* on ovarian cancer cellular behaviors is still uncertain. Among various human tumors, the oncogenic effects of *TOP2A* on cellular behavior in breast cancer are the most studied. As a downstream target of PTEN/AKT signaling, *TOP2A* was found to functionally promote cell growth and inhibit the cell apoptosis of breast cancer cells via ATP and caspase-3 signaling pathways (35). In addition, the mechanism by which *TOP2A* exerts aggressive properties in other cancers has been explored. In colon cancer, *TOP2A* enhanced cell proliferation and invasion ability via activating AKT and ERK pathway and phosphorylation of GSK-3β, which was correlated with the EMT process (36,37). Activation of the β-catenin pathway that is closely related to the EMT process may be the other novel mechanism by which *TOP2A* exerts aggressive properties in cancers, and this mechanism has been confirmed by research on pancreatic cancer (38). Our experiments demonstrated that silencing of *TOP2A* led to a promotive effect on ovarian cancer cell apoptosis, while a suppressive effect on proliferation, viability, adhesion and migration, which could be confidently restored by the introduction of miR-6884-5p inhibitor. Collectively, miR-6884-5p negatively regulated *TOP2A* to serve as a suppressor in ovarian cancer.

To date, we logically established the relationship among RHPN1-AS1, miR-6884-5p and *TOP2A* in ovarian cancer. As an oncogene in ovarian cancer, RHPN1-AS1 promoted ovarian carcinogenesis *in vitro*, possibly by sponging miR-6884-5p

to release *TOP2A*, the knockdown of which functionally increased cell apoptosis and impaired the capability of cell proliferation, viability, adhesion and migration in ovarian cancer. A limitation of this research is the lack of exploration on the downstream signaling pathway of *TOP2A*. In future study, the interaction between the AKT/ERK pathway and *TOP2A* as well as the β-catenin pathway and *TOP2A* could be investigated.

To conclude, lncRNA RHPN1-AS1 was identified as being overexpressed in ovarian cancer. According to our cellular behavioral experiments, RHPN1-AS1 reduced ovarian cancer cell apoptosis, and facilitated ovarian cancer cell proliferation, viability, adhesion and immigration through sponging miR-6884-5p and releasing *TOP2A*. Our findings suggest that RHPN1-AS1 could be a promising biomarker for novel therapeutic methods for ovarian cancer.

Acknowledgements

Not applicable.

Funding

No funding sources were utilized for this study.

Availability of data and materials

The data used and analyzed during the current study are available from the corresponding author on reasonable request.

Authors' contributions

Conceptualization, methodology, investigation, data analysis, and manuscript preparation were carried out by SC. Data analysis, visualization, resources, and manuscript preparation were carried out by FL.

Ethics approval and consent to participate

The study was approved by the Ethics Committee of Yantai Affiliated Hospital of Binzhou Medical University (approval no. 20190601001, Yantai, Shandong, China). All procedures performed in this study were in accordance with the 1964 Helsinki declaration. All patients provided written informed consent.

Patient consent for publication

Not applicable.

Competing interests

The authors declare that they have no competing interests.

References

1. Rottmann M, Burges A, Mahner S, Anthuber C, Beck T, Grab D, Schnelzer A, Kiechle M, Mayr D, Pölcher M, *et al*: Cancer of the ovary, fallopian tube, and peritoneum: A population-based comparison of the prognostic factors and outcomes. J Cancer Res Clin Oncol 143: 1833-1844, 2017.
2. Siegel RL, Miller KD and Jemal A: Cancer statistics, 2017. CA Cancer J Clin 67: 7-30, 2017.
3. Doubeni CA, Doubeni AR and Myers AE: Diagnosis and management of ovarian cancer. Am Fam Physician 93: 937-944, 2016.
4. Vaughan S, Coward JI, Bast RC Jr, Berchuck A, Berek JS, Brenton JD, Coukos G, Crum CC, Drapkin R, Etemadmoghadam D, *et al*: Rethinking ovarian cancer: Recommendations for improving outcomes. Nat Rev Cancer 11: 719-725, 2011.
5. Hoskins PJ and Gotlieb WH: Missed therapeutic and prevention opportunities in women with BRCA-mutated epithelial ovarian cancer and their families due to low referral rates for genetic counseling and BRCA testing: A review of the literature. CA Cancer J Clin 67: 493-506, 2017.
6. Cech TR and Steitz JA: The noncoding RNA revolution-trashing old rules to forge new ones. Cell 157: 77-94, 2014.
7. Kopp F and Mendell JT: Functional classification and experimental dissection of long noncoding RNAs. Cell 172: 393-407, 2018.
8. Schmitz SU, Grote P and Herrmann BG: Mechanisms of long noncoding RNA function in development and disease. Cell Mol Life Sci 73: 2491-2509, 2016.
9. Gupta RA, Shah N, Wang KC, Kim J, Horlings HM, Wong DJ, Tsai MC, Hung T, Argani P, Rinn JL, *et al*: Long non-coding RNA HOTAIR reprograms chromatin state to promote cancer metastasis. Nature 464: 1071-1076, 2010.
10. Huarte M, Guttman M, Feldser D, Garber M, Koziol MJ, Kenzelmann-Broz D, Khalil AM, Zuk O, Amit I, Rabani M, *et al*: A large intergenic noncoding RNA induced by p53 mediates global gene repression in the p53 response. Cell 142: 409-419, 2010.
11. Duan H, Li X, Chen Y, Wang Y and Li Z: LncRNA RHPN1-AS1 promoted cell proliferation, invasion and migration in cervical cancer via the modulation of miR-299-3p/FGF2 axis. Life Sci 239: 116856, 2019.
12. Ding L, Wang L, Li Z, Jiang X, Xu Y and Han N: The positive feedback loop of RHPN1-AS1/miR-1299/ETS1 accelerates the deterioration of gastric cancer. Biomed Pharmacother 124: 109848, 2020.
13. Zhang X, Yan Z, Wang L, Zhang S and Gao M: STAT1-induced upregulation of lncRNA RHPN1-AS1 predicts a poor prognosis of hepatocellular carcinoma and contributes to tumor progression via the miR-485/CDCA5 axis. J Cell Biochem: Feb 17, 2020 (Epub ahead of print).
14. Zheng W, Li H, Zhang H, Zhang C, Zhu Z, Liang H and Zhou Y: Long noncoding RNA RHPN1-AS1 promotes colorectal cancer progression via targeting miR-7-5p/OGT axis. Cancer Cell Int 20: 54, 2020.
15. Zheng S, Lv P, Su J, Miao K, Xu H and Li M: Silencing of the long non-coding RNA RHPN1-AS1 suppresses the epithelial-to-mesenchymal transition and inhibits breast cancer progression. Am J Transl Res 11: 3505-3517, 2019.
16. Li X, Zhang X, Yang C, Cui S, Shen Q and Xu S: The lncRNA RHPN1-AS1 downregulation promotes gefitinib resistance by targeting miR-299-3p/TNFSF12 pathway in NSCLC. Cell Cycle 17: 1772-1783, 2018.
17. Bartel DP: MicroRNAs: Target recognition and regulatory functions. Cell 136: 215-233, 2009.
18. Bartel DP: MicroRNAs: Genomics, biogenesis, mechanism, and function. Cell 116: 281-297, 2004.
19. Pasquinelli AE: MicroRNAs and their targets: Recognition, regulation and an emerging reciprocal relationship. Nat Rev Genet 13: 271-282, 2012.
20. Esquela-Kerscher A and Slack FJ: Oncomirs-microRNAs with a role in cancer. Nat Rev Cancer 6: 259-269, 2006.
21. Lv H, Hou H, Lei H, Nie C, Chen B, Bie L, Han L and Chen X: MicroRNA-6884-5p regulates the proliferation, invasion, and EMT of gastric cancer cells by directly targeting S100A16. Oncol Res 28: 225-236, 2020.
22. Beltrame L, Di Marino M, Fruscio R, Calura E, Chapman B, Clivio L, Sina F, Mele C, Iatropoulos P, Grassi T, *et al*: Profiling cancer gene mutations in longitudinal epithelial ovarian cancer biopsies by targeted next-generation sequencing: A retrospective study. Ann Oncol 26: 1363-1371, 2015.
23. Erriquez J, Becco P, Olivero M, Ponzone R, Maggiorotto F, Ferrero A, Scalzo MS, Canuto EM, Sapino A, Verdun di Cantogno L, *et al*: TOP2A gene copy gain predicts response of epithelial ovarian cancers to pegylated liposomal doxorubicin: TOP2A as marker of response to PLD in ovarian cancer. Gynecol Oncol 138: 627-633, 2015.

24. Sherman-Baust CA, Kuhn E, Valle BL, Shih IeM, Kurman RJ, Wang TL, Amano T, Ko MS, Miyoshi I, Araki Y, *et al*: A genetically engineered ovarian cancer mouse model based on fallopian tube transformation mimics human high-grade serous carcinoma development. J Pathol 233: 228-237, 2014.
25. Dong S, Wang R, Wang H, Ding Q, Zhou X, Wang J, Zhang K, Long Y, Lu S, Hong T, *et al*: HOXD-AS1 promotes the epithelial to mesenchymal transition of ovarian cancer cells by regulating miR-186-5p and PIK3R3. J Exp Clin Cancer Res 38: 110, 2019.
26. Shahab SW, Matyunina LV, Mezencev R, Walker LD, Bowen NJ, Benigno BB and McDonald JF: Evidence for the complexity of microRNA-mediated regulation in ovarian cancer: A systems approach. PLoS One 6: e22508, 2011.
27. Edgar R, Domrachev M and Lash AE: Gene Expression Omnibus: NCBI gene expression and hybridization array data repository. Nucleic Acids Res 30: 207-210, 2002.
28. Livak KJ and Schmittgen TD: Analysis of relative gene expression data using real-time quantitative PCR and the 2(-Delta Delta C(T)) method. Methods 25: 402-408, 2001.
29. Zhao J, Yang T, Ji J, Zhao F, Li C and Han X: RHPN1-AS1 promotes cell proliferation and migration via miR-665/Akt3 in ovarian cancer. Cancer Gene Ther 28: 33-41, 2020.
30. Wang J, Ding W, Xu Y, Tao E, Mo M, Xu W, Cai X, Chen X, Yuan J and Wu X: Long non-coding RNA RHPN1-AS1 promotes tumorigenesis and metastasis of ovarian cancer by acting as a ceRNA against miR-596 and upregulating LETM1. Aging (Albany NY) 12: 4558-4572, 2020.
31. Tao F, Tian X, Lu M and Zhang Z: A novel lncRNA, Lnc-OC1, promotes ovarian cancer cell proliferation and migration by sponging miR-34a and miR-34c. J Genet Genomics 45: 137-145, 2018.
32. Zou MF, Ling J, Wu QY and Zhang CX: Long non-coding RNA PVT1 functions as an oncogene in ovarian cancer via upregulating SOX2. Eur Rev Med Pharmacol Sci 22: 7183-7188, 2018.
33. Wang Q, Li XP, Zhou X, Yang CF and Zhu Z: A single-nucleotide polymorphism in lnc-LAMC2-1:1 interferes with its interaction with miR-128 to alter the expression of deleted in colorectal cancer and its effect on the survival rate of subjects with ovarian cancer. J Cell Biochem 121: 4108-4119, 2020.
34. Nuncia-Cantarero M, Martinez-Canales S, Andres-Pretel F, Santpere G, Ocana A and Galan-Moya EM: Functional transcriptomic annotation and protein-protein interaction network analysis identify NEK2, BIRC5, and TOP2A as potential targets in obese patients with luminal A breast cancer. Breast Cancer Res Treat 168: 613-623, 2018.
35. Yang Z, Liu Y, Shi C, Zhang Y, Lv R, Zhang R, Wang Q and Wang Y: Suppression of PTEN/AKT signaling decreases the expression of TUBB3 and TOP2A with subsequent inhibition of cell growth and induction of apoptosis in human breast cancer MCF-7 cells via ATP and caspase-3 signaling pathways. Oncol Rep 37: 1011-1019, 2017.
36. Zhao J, Ou B, Han D, Wang P, Zong Y, Zhu C, Liu D, Zheng M, Sun J, Feng H and Lu A: Tumor-derived CXCL5 promotes human colorectal cancer metastasis through activation of the ERK/Elk-1/Snail and AKT/GSK3β/β-catenin pathways. Mol Cancer 16: 70, 2017.
37. Zhou SL, Zhou ZJ, Hu ZQ, Li X, Huang XW, Wang Z, Fan J, Dai Z and Zhou J: CXCR2/CXCL5 axis contributes to epithelial-mesenchymal transition of HCC cells through activating PI3K/Akt/GSK-3β/Snail signaling. Cancer Lett 358: 124-135, 2015.
38. Pei YF, Yin XM and Liu XQ: TOP2A induces malignant character of pancreatic cancer through activating β-catenin signaling pathway. Biochim Biophys Acta Mol Basis Dis 1864: 197-207, 2018.